Radiocarbon, Vol 66, Nr 2, 2024, p 386–399 DOI:10.1017/RDC.2024.27
© The Author(s), 2024. Published by Cambridge University Press on behalf of University of Arizona. This is an Open Access article, distributed under the terms of the Creative Commons Attribution licence (http://creativecommons.org/licenses/by/4.0/), which permits unrestricted re-use, distribution and reproduction, provided the original article is properly cited.

DISCUSSION: PRESENTATION OF ATMOSPHERIC $^{14}CO_2$ DATA

Stephen E Schwartz[1]* • Quan Hua[2] • David E Andrews[3] • Ralph F Keeling[4] • Scott J Lehman[5] • Jocelyn C Turnbull[6] • Paula J Reimer[7] • John B Miller[8] • Harro A J Meijer[9]

[1]School of Marine and Atmospheric Sciences, Stony Brook University, Stony Brook, NY 11974, USA
[2]Australian Nuclear Science and Technology Organisation, Locked Bag 2001, Kirrawee DC, NSW 2232, Australia; School of Social Science, University of Queensland, Brisbane, QLD 4072, Australia
[3]Department of Physics and Astronomy, University of Montana, Missoula, MT, USA
[4]Scripps Institution of Oceanography, University of California, San Diego, La Jolla, CA 92093, USA
[5]INSTAAR, University of Colorado, Boulder, CO 80309-0450, USA
[6]Rafter Radiocarbon Laboratory, GNS Science, Lower Hutt, New Zealand; CIRES, University of Colorado, Boulder, CO, USA
[7]CHRONO Centre for Climate, the Environment and Chronology, School of Natural and Built Environment, Department of Geography, Archaeology and Palaeoecology, Queen's University Belfast BT7 1NN, United Kingdom
[8]NOAA Global Monitoring Laboratory, Boulder, Colorado, USA
[9]Centre for Isotope Research (CIO), Energy and Sustainability Research Institute Groningen, University of Groningen, Groningen, Netherlands

ABSTRACT. Observations of radiocarbon (^{14}C) in Earth's atmosphere and other carbon reservoirs are important to quantify exchanges of CO_2 between reservoirs. The amount of ^{14}C is commonly reported in the so-called Delta notation, i.e., $\Delta^{14}C$, the decay- and fractionation-corrected departure of the ratio of ^{14}C to total C from that ratio in an absolute international standard; this Delta notation permits direct comparison of $^{14}C/C$ ratios in the several reservoirs. However, as $\Delta^{14}C$ of atmospheric CO_2, $\Delta^{14}CO_2$ is based on the ratio of $^{14}CO_2$ to total atmospheric CO_2, its value can and does change not just because of change in the amount of atmospheric $^{14}CO_2$ but also because of change in the amount of total atmospheric CO_2, complicating ascription of change in $\Delta^{14}CO_2$ to change in one or the other quantity. Here we suggest that presentation of atmospheric $^{14}CO_2$ amount as mole fraction relative to dry air (moles of $^{14}CO_2$ per moles of dry air in Earth's atmosphere), or as moles or molecules of $^{14}CO_2$ in Earth's atmosphere, all readily calculated from $\Delta^{14}CO_2$ and the amount of atmospheric CO_2 (with slight dependence on $\delta^{13}CO_2$), complements presentation only as $\Delta^{14}CO_2$, and can provide valuable insight into the evolving budget and distribution of atmospheric $^{14}CO_2$.

KEYWORDS: $^{14}CO_2$, abundance, atmosphere, mixing ratio, radiocarbon.

MOTIVATION AND EXAMPLES

The amount of radiocarbon in atmospheric carbon dioxide ($^{14}CO_2$) is of fundamental importance to inference of the budget of radiocarbon and atmospheric CO_2 and of natural and anthropogenic changes in both quantities; here the term "amount" denotes any measure of the quantity of the substance under consideration. Historically the use of radiocarbon to infer the extent of anthropogenic perturbation of the amount of atmospheric CO_2 goes back to Suess (1955), who famously demonstrated the decrease in $^{14}C/C$ of atmospheric $^{14}CO_2$ with time over the nineteenth century as inferred from dendrochronologically dated wood samples; this decrease was attributed to emissions into the atmosphere of ^{14}C-free CO_2 from fossil fuel combustion. Although Suess recognized that the magnitude of the perturbation of $^{14}C/C$ would be decreased by exchange of atmospheric CO_2 with the oceans (what is now characterized as "disequilibrium isotope flux"), he underestimated by an order of magnitude the extent of increase of what he characterized as "contamination of Earth's atmosphere by artificial CO_2." Nonetheless that work set the scene for use of $^{14}CO_2$ to infer the extent of such exchange.

*Corresponding author. Email: stephen.schwartz@stonybrook.edu

https://doi.org/10.1017/RDC.2024.27 Published online by Cambridge University Press

Historically and at present the $^{14}C/C$ ratio of atmospheric CO_2 has been reported most commonly as $\Delta^{14}CO_2$, the depletion or enrichment of ^{14}C in sample relative to an internationally accepted absolute reference standard, normalized for mass-dependent isotope fractionation and corrected for decay from date of sampling (atmospheric CO_2) or of growth (tree rings), i.e., the quantity denoted Δ by Stuiver and Polach (1977), commonly presented in parts per thousand or "per mil." The use of per mil notation reflects the generally small differences of fractionation- and decay-corrected relative $^{14}C/C$ ratio in different ambient carbon reservoirs and the gradients within these reservoirs that result from relatively small perturbations together with rather rapid redistribution of ^{14}C via air-sea gas exchange, photosynthesis and respiration, and physical mixing. Much larger differences and gradients occur when the system is substantially perturbed. Such perturbations have included the large excess of $^{14}CO_2$ originating from above-ground testing of nuclear weapons in the 1950s and early 1960s (commonly referred to as "bomb radiocarbon") and the anomalously high natural production of ^{14}C and dramatically altered carbon cycle dynamics during the last ice age (Hughen et al. 2004).

The decrease in $\Delta^{14}C$ of atmospheric CO_2 that had been discovered by Suess (1955) from just a handful of tree-ring samples was examined much more systematically by Stuiver and colleagues (Stuiver and Quay 1981; Stuiver et al. 1998), again using dendrochronologically determined ages and is presented as $\Delta^{14}CO_2$, as is conventional, in Figure 1a. Figure 1b shows the time series of the amount of atmospheric $^{14}CO_2$ in the global atmosphere as mole fraction relative to dry air, x_{14CO2}. Figure 1c shows the time series of the mole fraction of CO_2 in Earth's atmosphere x_{CO2}. Here the designation of the several time series in Figure 1 as representative of the global atmosphere should be qualified as approximate, as the quantities $\Delta^{14}CO_2$, x_{CO2}, and x_{14CO2}, are obtained from measurements at different locations and thus do not take into account slight spatial variation.

Conversion of measured $\Delta^{14}CO_2$ to x_{14CO2} is quite straightforward by Eq. (1),

$$x_{14CO2} = f\left[\frac{1+\delta^{13}CO_2}{1-0.025}\right]^2(1+\Delta^{14}CO_2)x_{CO2}, \tag{1}$$

provided that the associated CO_2 mole fraction, x_{CO2}, is also known, as developed in Appendix A; the factor $f = 1.176 \times 10^{-12}$. The conversion is also weakly dependent on $\delta^{13}CO_2$ to account for mass-dependent fractionation. The mole fraction x_{14CO2} is entirely analogous to the commonly used mole fraction of CO_2 itself, x_{CO2}, typically expressed as ppm $\equiv$ μmol mol^{-1}, and to mole fractions of other trace gases in the global atmosphere (ppm, ppb etc.), all relative to the amount of dry air. In view of the magnitude of x_{14CO2} it would seem convenient to express x_{14CO2} in the unit amol mol^{-1}, where amol (attomole) is 10^{-18} mol. This measure of the amount of $^{14}CO_2$ is denoted here as an absolute measure, as distinguished from the relative measure, i.e., $\Delta^{14}CO_2$, in which the amount of $^{14}CO_2$ is expressed relative to the amount of CO_2. The mole fraction of $^{14}CO_2$ (or any other gas) in Earth's atmosphere is readily converted to moles by means of the essentially constant amount of air in the dry global atmosphere (1.765×10^{20} moles, uncertain to 0.5%; Prather et al. 2012) or to molecules, by further use of the Avogadro constant.

The time series for $\Delta^{14}CO_2$ and x_{14CO2} in Figures 1a and b show an important qualitative difference between these two measures of the amount of $^{14}CO_2$ in Earth's atmosphere. In contrast to the familiar decrease of $\Delta^{14}CO_2$ with time (Figure 1a), x_{14CO2} yields a very different picture (Figure 1b), that of a systematic *increase*. The reason for the qualitatively different

https://doi.org/10.1017/RDC.2024.27 Published online by Cambridge University Press

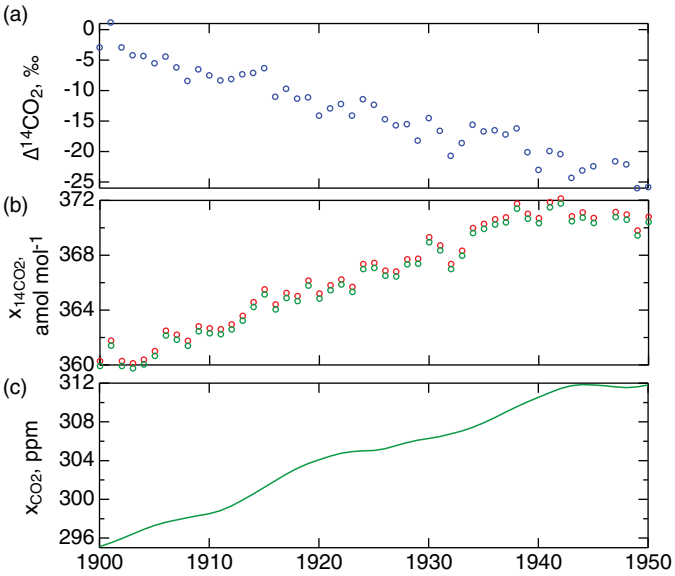


Figure 1 Alternative presentations of the amount of $^{14}CO_2$ in the global atmosphere over the first half of the twentieth century: *a*, as departure (in units of parts per thousand, "per mil," ‰) of the ratio of $^{14}CO_2$ to total CO_2 in the atmosphere corrected for fractionation and year of growth from the ratio of ^{14}C to C in the absolute standard, $\Delta^{14}CO_2$ (samples from Douglas Fir and Noble Fir trees from the US Pacific Northwest (43°7'–47°46'N, 121°45'–124°06'W), and an Alaskan Sitka spruce tree (58°N, 153°W); data tabulated in Stuiver et al. 1998); and *b*, as mole fraction (mole $^{14}CO_2$ per mole of dry air), x_{14CO2}; the unit amol/mol denotes part per 10^{18}. Red points denote values calculated with observation-derived $\delta^{13}CO_2$ (fit to data of Francey et al. (1999), Appendix B, Figure B2); green points denote values calculated for $\delta^{13}CO_2$ taken as constant, –7‰. *c*, Mole fraction of atmospheric CO_2 (mole CO_2 per mole of dry air), x_{CO2}, in units of parts per million, ppm (data from Law Dome, Antarctica; Etheridge et al. 1996). Because of limited spatial coverage of the measurements the quantities shown should be considered only approximate global averages.

picture in the time series is the substantial increase of total atmospheric CO_2 over the same time period (Figure 1c). The relative increase in CO_2 mole fraction x_{CO2} over this time period, ~5%, outweighs the relative decrease in $1 + \Delta^{14}CO_2$ [i.e., $1 + \Delta^{14}CO_2$(‰)/1000(‰)], ~25‰ (Stuiver and Polach 1977) or ~2.5%, the measure of $^{14}CO_2$ amount that enters into the calculation of absolute amount, resulting in the increase in x_{14CO2} of ~2.8%. The strong influence of the increase of x_{CO2}, on x_{14CO2}, is apparent in the near congruence of the time profiles of these quantities. A strength of x_{14CO2} as a measure of $^{14}CO_2$ amount is that as an absolute measure of amount as opposed to a relative measure, that is, relative to the amount of atmospheric CO_2, it is not influenced by the increase of CO_2 amount over this time period.

Emission of fossil-fuel CO_2 over the first half of the twentieth century has affected the evolution of both $\Delta^{14}CO_2$ and x_{14CO2}. $\Delta^{14}CO_2$ (or $^{14}C/C$ ratio) has decreased mainly because of the increase in the atmospheric inventory of ^{14}C-free CO_2 from fossil fuel combustion. In contrast, x_{14CO2} has increased mainly because the increase in ^{14}C-free CO_2 in the atmosphere has induced isotopic exchange with carbon in the ^{14}C-containing ocean and terrestrial reservoirs that has resulted in net transfer of $^{14}CO_2$ into the atmosphere, resulting in increase in x_{14CO2} over this period. Here it might also be noted that x_{14CO2} is only weakly dependent on $\delta^{13}CO_2$, the dependence manifested as the difference between the red points in Figure 3b calculated for observation-derived values of $\delta^{13}CO_2$, and the green points calculated for $\delta^{13}CO_2$ taken as constant, –7‰.

https://doi.org/10.1017/RDC.2024.27 Published online by Cambridge University Press

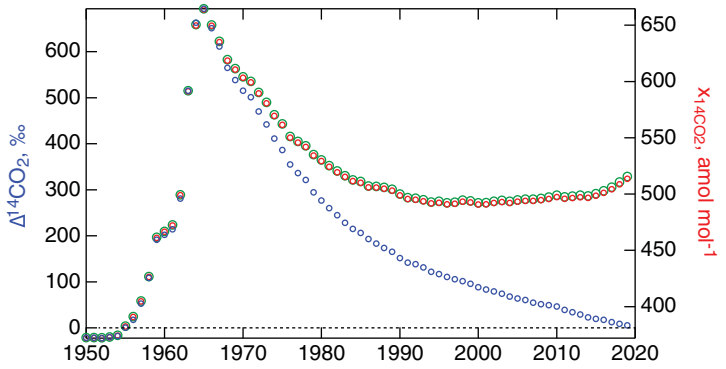


Figure 2 Alternative presentations of the amount of $^{14}CO_2$ in the global atmosphere over the second half of the twentieth century to the present, as departure of the ratio of $^{14}CO_2$ to total CO_2 in the atmosphere from that ratio in the absolute standard, $\Delta^{14}CO_2$, blue, left axis (Hua et al. 2022); and as mole fraction relative to dry air x_{14CO2}, red, right axis. Values of x_{CO2} needed to calculate x_{14CO2} are from measurements in ice cores at Law Dome, Antarctica and air at Cape Grim, Tasmania (Etheridge et al. 1996) and from measurements in air (Keeling et al. 1976, 2001 as updated, and Ballantyne et al. 2017 as updated by Dlugokencky and Tans 2018) as tabulated by Le Quéré et al. (2018). Values of $\delta^{13}CO_2$ used to calculate x_{14CO2} are from a linear fit to data of Francey et al. (1999), shown in Appendix B, Figure B1; also shown, larger green markers, right axis, are values of x_{14CO2} calculated with $\delta^{13}CO_2$ taken as constant, –7‰. Because of limited spatial coverage of the measurements the quantities shown should be considered approximate rather than true global averages.

A second example of the qualitative difference between time series of radiocarbon amount expressed as $\Delta^{14}CO_2$ and x_{14CO2} is manifested in Figure 2 for the period during and after the introduction of excess radiocarbon from above-ground nuclear weapons testing. This testing resulted in a large increase in atmospheric $^{14}CO_2$ over the time period 1955–1964 (e.g., Levin et al. 1985, 2010; Turnbull et al. 2017). Following nearly complete cessation of testing in 1964 the amount of atmospheric $^{14}CO_2$ rather rapidly decreased, mainly because of isotopic exchange with other reservoirs in the carbon system. $\Delta^{14}CO_2$ exhibits a monotonic decrease from its peak value in the early 1960s that continues up to the present time. Also shown in the figure is x_{14CO2}, as calculated by Eq. (1). In contrast to $\Delta^{14}CO_2$, x_{14CO2} reached a minimum around 2000, increasing thereafter. This contrast in the time series of the relative and absolute amounts of $\Delta^{14}CO_2$ versus x_{14CO2} over this time period, presented recently also by Andrews (2020) and Andrews and Tans (2022), highlights the distinction between these two measures of the amount of $^{14}CO_2$ in Earth's atmosphere.

As shown in Figure 2, $\Delta^{14}CO_2$ is now decreasing below zero, the approximate value in the preindustrial atmosphere. $\Delta^{14}CO_2$ can be expected to continue to decrease because of continued emissions of ^{14}C–free CO_2 from fossil fuel combustion. In contrast, x_{14CO2}, already increasing subsequent to about year 1995, would be expected to continue to increase, mainly because isotopic equilibration results in net transfer of ^{14}C from the ocean and the terrestrial biosphere into the atmosphere in response to the increasing amount of ^{14}C–free atmospheric CO_2, together with slight emissions of $^{14}CO_2$ from nuclear power production.

A third example deals with differences in amounts of atmospheric $^{14}CO_2$ between the Northern and Southern Hemispheres as quantified by x_{14CO2} versus $\Delta^{14}CO_2$. The differences in $\Delta^{14}CO_2$ were examined by Levin et al. (2010) and Graven et al. (2012), with the finding that subsequent to about year 2000, $\Delta^{14}CO_2$ in the Southern Hemisphere (SH) systematically exceeded that in the Northern Hemisphere (NH). Examining hemispheric and sub-hemispheric measurements

https://doi.org/10.1017/RDC.2024.27 Published online by Cambridge University Press

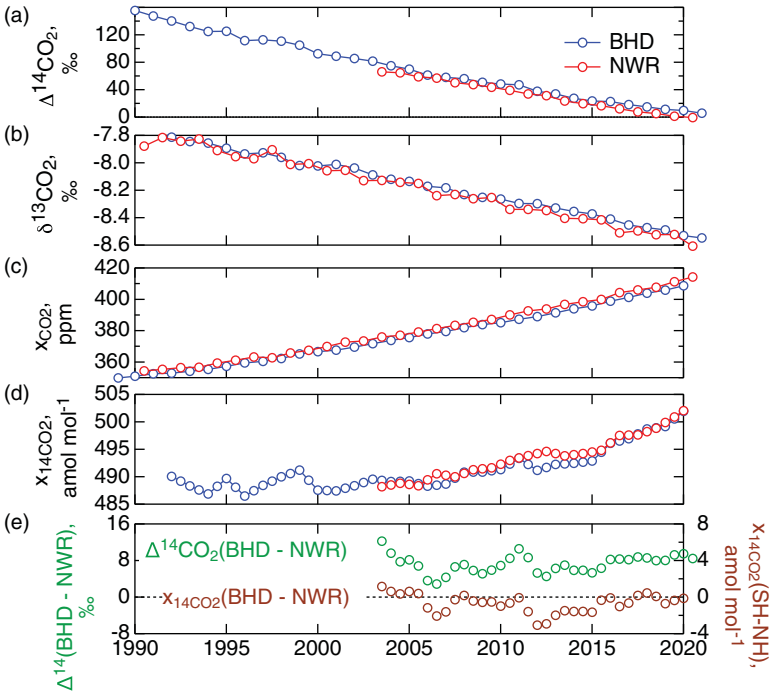


Figure 3 Comparison of alternative presentations of atmospheric $^{14}CO_2$ amount and controlling quantities in Northern and Southern Hemisphere summers. *a*, $\Delta^{14}CO_2$, at Niwot Ridge (NWR, Colorado, USA) for summer months (May-August) in the NH and at Baring Head (BHD, New Zealand) in the SH (November-February), similar to Hua et al. (2022). *b*, $\delta^{13}CO_2$. *c*, x_{CO2}. *d*, x_{14CO2}; *e*, difference in $\Delta^{14}CO_2$ and x_{14CO2} between the BHD and NWR sites.

in the summer months in each hemisphere, Hua et al. (2022) similarly found that over this time period $\Delta^{14}CO_2$ in the SH was systematically greater than in the NH. The data examined here in Figure 3 for the summer months (in the two hemispheres) of years 1990–2020 at specific locations, Niwot Ridge (NWR, Colorado, USA; Lehman et al. 2013, updated) in the NH and Baring Head (BHD, New Zealand; Turnbull et al. 2017, updated) in the SH, likewise show systematically greater $\Delta^{14}CO_2$ in the SH, Figure 3a. However, a different picture emerges for x_{14CO2}, Figure 3d (for some years for which x_{14CO2} could not be derived from BHD measurements, measurements at Cape Grim Observatory, Tasmania, Australia (Levin et al. 1996, 1999, 2011; Turnbull et al. 2017) were substituted). In contrast to $\Delta^{14}CO_2$, x_{14CO2} was comparable to or even slightly greater at the NH site than at the SH site. Figure 3e presents differences between $\Delta^{14}CO_2$ and x_{14CO2} at the two sites; as the summertime measurements are staggered by half a year, the differences were taken for values obtained by interpolation. These differences explicitly show that whereas summertime $\Delta^{14}CO_2$ at BHD systematically exceeds that at NWR, values of x_{14CO2} at BHD are essentially the same as, or less than those at NWR over this time period; that is, a difference, even in sign, between the interhemispheric differences of $\Delta^{14}CO_2$ versus x_{14CO2}.

PRIOR PRESENTATION OF ABSOLUTE AMOUNT OF ATMOSPHERIC $^{14}CO_2$

Although the amount of atmospheric $^{14}CO_2$ has most commonly been presented as $\Delta^{14}CO_2$, there are more than a few precedents in which this amount has been presented as an absolute

https://doi.org/10.1017/RDC.2024.27 Published online by Cambridge University Press

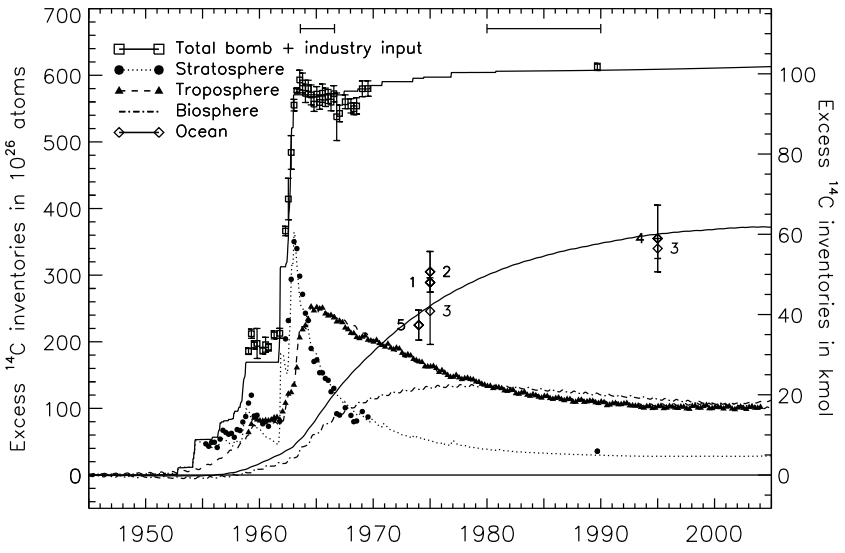


Figure 4 Evolution of the inventories of anthropogenic radiocarbon in the stratosphere, the troposphere, the world ocean, and the terrestrial biosphere, as given by Naegler and Levin (2006); units are 10^{26} atoms (left ordinate) and kmol (right ordinate). Solid line denotes estimated total production amount based on the Yang et al. (2000) compilation of atmospheric nuclear detonation. Symbols denote measurements; for identification see the original paper. Curves denote modeled amounts in the several reservoirs. Reproduced with permission of the American Geophysical Union.

quantity (number of molecules or moles in the global atmosphere). Much of this usage has been to examine the disposition of bomb radiocarbon, where use of absolute amount permits comparison of the total bomb yield of ^{14}C with the amounts in the global atmosphere, the world ocean, and the terrestrial biosphere, (e.g., Levin and colleagues (Hesshaimer et al. 1994; Naegler and Levin 2006: their Figure 4a reproduced here as Figure 4); Broecker et al. 1995; Lassey et al. 1996; Joos and Bruno 1998; Caldeira et al. 1998; Key et al. 2004; Peacock 2004; Mouchet 2013) or comparison just of amounts in the several reservoirs (Graven 2015: figure S1).

In another application Roth and Joos (2013, their Figure 2, modified and presented here as Figure 5), examined the rate of natural production of ^{14}C and the disposition of this ^{14}C among the several geophysical reservoirs and its distribution under the influence of a changing carbon cycle. Those investigators presented the amount of $^{14}CO_2$ in the global atmosphere over the past 21 kyr both as $\Delta^{14}CO_2$ and as absolute amount (moles of $^{14}CO_2$ in the global atmosphere). Comparison of the two time series shows that the absolute amount over this time period was more or less constant, in contrast to $\Delta^{14}CO_2$, which exhibited a substantial systematic decrease. The decrease in $\Delta^{14}CO_2$ must therefore be ascribed largely to increase in the amount of atmospheric CO_2; this is confirmed by the rather close conformance of $\Delta^{14}CO_2$ and CO_2 mole fraction x_{CO2}, the latter shown on an inverted scale. The relative constancy of $^{14}CO_2$ inventory that results from the cancellation of these trends has also been noted by Köhler et al. (2022; Figure 1c), who stress the central role of the trend of the amount of atmospheric CO_2 as the source of the trend in $\Delta^{14}CO_2$ over this time period.

https://doi.org/10.1017/RDC.2024.27 Published online by Cambridge University Press

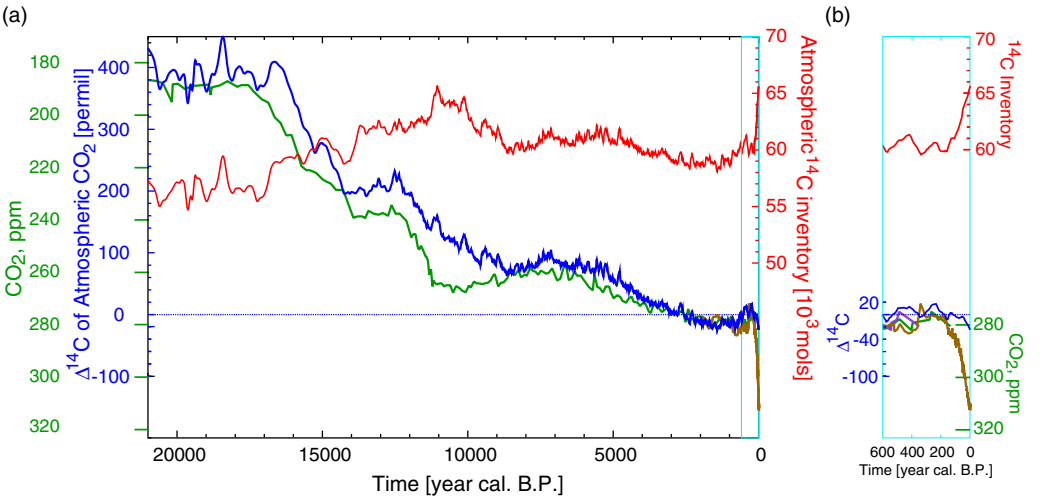


Figure 5 *a*. Reconstructed $\Delta^{14}C$ of atmospheric CO_2 (blue, left axis) and absolute inventory of atmospheric radiocarbon (red, right axis) over the past 21 kyr, modified from Figure 2 of Roth and Joos (2013). Added to the figure, far left axis (inverted scale), is mole fraction of atmospheric CO_2 inferred from the EPICA Dome (Antarctica) ice core (Bereiter et al. 2015), green, and from multiple ice cores (MacFarling Meure 2004; MacFarling Meure et al. 2006; Etheridge et al. 1996 as tabulated by Etheridge et al. 2010), brown, again on an inverted scale. *b*. Last 600 years of the several time series, denoted by cyan rectangle in *a*, with 5-fold expansion of horizontal scale.

Although not explicitly noted by Roth and Joos, the increase in the absolute amount of $^{14}CO_2$ inventory over the first half of the twentieth century (shown above in Figure 1b) is evident also in the most recent part of the data presented by those investigators (50 to 0 year cal. BP), shown on an expanded time scale in Figure 5b, along with the increase in mole fraction of atmospheric CO_2 and near constancy of $\Delta^{14}CO_2$ over this time period.

Reporting amounts of radiocarbon in terms of absolute amount rather than as departure from a standard is not uncommon in other contexts, for example the amount of ^{14}CO in the global atmosphere (Jöckel et al. 2002; Manning et al. 2005; Hmiel et al. 2020).

DISCUSSION

Based on the examples presented it is suggested here that presentation of $^{14}CO_2$ amount as x_{14CO2} readily allows assessment of time trends or spatial gradients of $^{14}CO_2$ amount and that such presentation, alongside $\Delta^{14}CO_2$, the directly measured and more widely presented measure of $^{14}CO_2$ amount in the atmosphere, may lend additional insight. Importantly, the roughly constant value of x_{14CO2} between 1995 and 2010 shown in Figure 2 shows that in these years loss of $^{14}CO_2$ from the atmosphere was closely balanced by addition, whereas earlier, the amount of $^{14}CO_2$ in the atmosphere had been decreasing, and at present that amount is increasing. This situation is not at all evident in the time trace of $\Delta^{14}CO_2$, which shows monotonic decrease over this period.

On the other hand, presentation of atmospheric $^{14}CO_2$ data as $\Delta^{14}CO_2$ readily permits examination of time series of the departure from isotopic equilibrium between atmospheric $^{14}CO_2$ and ^{14}C in other reservoirs. For example, Andrews et al. (2016) and Wu et al. (2021) compared time series of $\Delta^{14}CO_2$ with time series of $\Delta^{14}C$ in the oceanic mixed layer (ML), the

https://doi.org/10.1017/RDC.2024.27 Published online by Cambridge University Press

latter as determined from measurements of $\Delta^{14}C$ in dated coral and fish otolith samples and directly in ML water samples in the North and South Pacific Gyres.

A key motivation of study of the amount of $^{14}CO_2$ in the global atmosphere is qualitative and quantitative understanding of the processes that govern the changes in this amount and the amounts of ^{14}C in other reservoirs of the biogeosphere. In some contexts process understanding is enhanced by presenting and examining the amount of atmospheric $^{14}CO_2$ as absolute amount, as quantified by atoms, moles, or mole fraction in air (x_{14CO2}), in addition to relative amount, as quantified by departure of isotopic ratio from the absolute standard, in $\Delta^{14}C$ units. As noted above (Figure 4) examination of absolute amount permits immediate comparison of the amounts of ^{14}C in different reservoirs of the biogeosphere. This comparison has been of great value in understanding the disposition of the bomb perturbation. Likewise, examination of time series of x_{14CO2} yields a picture of the temporal evolution of the amount of $^{14}CO_2$ in the global atmosphere that is qualitatively different from that exhibited by time series of $\Delta^{14}CO_2$, which is influenced by changes in amounts of both $^{14}CO_2$ and total CO_2.

In other contexts expressing the amount of ^{14}C in $\Delta^{14}C$ units also promotes process-level understanding. As the relative amount of ^{14}C in a sample is based on the activity of the sample relative to that of a standard, or its equivalent determined by accelerator mass spectrometry (AMS), it is appropriate that for geochemical samples this amount be reported as the fractionation- and decay-corrected $\Delta^{14}C$ (the quantity Δ of Stuiver and Polach 1977; Stuiver 1980) or as fractionation-corrected fraction modern (the quantity $F^{14}C$ of Reimer et al. 2004; Millard 2014). Under the condition of isotopic equilibrium, the several reservoirs of the biogeosphere (e.g., atmosphere, ocean, terrestrial biosphere) will all, in the absence of appreciable decay, exhibit the same $\Delta^{14}C$ values or will exhibit $\Delta^{14}C$ values that differ by a simple expression that accounts for decay and turnover time. A major driver of changes in atmospheric radiocarbon is thus isotopic disequilibrium with the oceans and the land biosphere. For example, how might the increase in the mole fraction of atmospheric $^{14}CO_2$ that arises from adding radiocarbon-free CO_2 to the atmosphere, as in Figure 1b, be understood? Using $\Delta^{14}C$ units provides a straightforward qualitative answer: the increase results from upsetting the preindustrial isotopic equilibrium causing, e.g., ecosystem respiration to be "hotter" than photosynthesis, i.e., characterized by a greater $\Delta^{14}C$ value. The disequilibrium flux and concomitant impact on $\Delta^{14}CO_2$ stop when the $\Delta^{14}C$ values converge between the reservoirs. Similarly, how might the controls on the interhemispheric gradient or the long-term trend in radiocarbon be understood? The answer is again relatively simple from a $\Delta^{14}C$ perspective: the dominant controls are fossil-fuel burning and the disequilibrium fluxes. Additionally, much of the variability imposed by the land biosphere net fluxes (i.e., net ecosystem exchange) conveniently drops out because of the ^{13}C normalization. Hence, because of the important contribution from disequilibrium fluxes, an understanding of the controls on the mole fraction of atmospheric radiocarbon sensibly starts with understanding of the controls on $\Delta^{14}C$.

As x_{14CO2} obtained from measured $\Delta^{14}CO_2$ by Eq. (1) is proportional to x_{CO2}, it is essential that the value of x_{CO2} used in the conversion be specified. Although, as shown in Figure 2, x_{14CO2} calculated with $\delta^{13}C$ taken as constant –7‰ is quite accurate, it may be necessary in precise work to use the concurrently measured value of $\delta^{13}C$, Figure 3. Hence it is recommended that when x_{14CO2} is presented, the value of $\delta^{13}C$ used in the conversion be presented. The uncertainty associated with x_{14CO2} is readily determined from propagation of uncertainties in Eq. (1).

https://doi.org/10.1017/RDC.2024.27 Published online by Cambridge University Press

At the end of the day, is one means of expressing amounts of $^{14}CO_2$, "better" or more suitable than the other? It is not clear that there is an unambiguous answer. It would seem that for studies examining the consequences of addition of fossil fuel CO_2 to the atmosphere, use of $\Delta^{14}C$ values might be more appropriate, because it is not necessary to know the amount of CO_2 precisely (which amount may not be known, particularly when ^{14}C content is derived from plant material or NaOH absorption samples). On the other hand, for modeling studies, absolute amounts (x_{CO2}, x_{13CO2}, and x_{14CO2}) might be more suitable because these quantities are measures of what actually gets transported. Also, especially in time series of the amount of atmospheric $^{14}CO_2$, absolute amount (mole fraction) presents the actual change in the amount of $^{14}CO_2$ in the atmosphere as opposed to relative amount (isotope ratio), which can be influenced more by change in the amount of total CO_2 than by change in the amount of $^{14}CO_2$.

AUTHOR CONTRIBUTIONS

This discussion paper was stimulated by discussion among several authors (DA, RFK, HAJM, SES, JCT) arising out of comments (Andrews and Tans 2022; Schwartz et al. 2022) on a publication that had misinterpreted the rate of decrease of atmospheric bomb $^{14}CO_2$ as a measure of the rate of removal of anthropogenic CO_2 from the biogeosphere. SES prepared the initial draft and figures and led revisions. QH provided data for Figure 3. All authors contributed to preparation and revision of the manuscript.

ACKNOWLEDGMENTS

We thank the Editors and three Reviewers for valuable comments and suggestions. Work by SES was conducted mainly while at Brookhaven National Laboratory and supported in part by the US Department of Energy under Contract No. DE-SC0012704; views expressed here do not necessarily represent the views of BNL or DOE.

SUPPLEMENTARY MATERIAL

To view supplementary material for this article, please visit https://doi.org/10.1017/RDC.2024.27.

REFERENCES

Andrews AH, Siciliano D, Potts DC, DeMartini EE, Covarrubias S. 2016. Bomb radiocarbon and the Hawaiian Archipelago: coral, otoliths, and seawater. Radiocarbon 58(3):531–548.

Andrews DE. 2020. Correcting an error in some interpretations of atmospheric ^{14}C data. Earth Sciences 9(4):126–129.

Andrews DE, Tans P. 2022. Comments on Skrable et al. (2022). Health Physics 122:707–709. https://journals.lww.com/health-physics/fulltext/2022/06000/comments_on_skrable_et_al___2022_.7.aspx

Ballantyne A, Smith W, Anderegg W, Kauppi P, Sarmiento J, Tans P, Shevliakova E, Pan Y, Poulter B, Anav A, Friedlingstein P. 2017. Accelerating net terrestrial carbon uptake during the warming hiatus due to reduced respiration. Nature Climate Change 7:148–152. https://www.nature.com/articles/nclimate3204

Bereiter B, Eggleston S, Schmitt J, Nehrbass-Ahles C, Stocker TF, Fischer H, Kipfstuhl S, Chappellaz J. 2015. Revision of the EPICA Dome C CO_2 record from 800 to 600 kyr before present. Geophysical Research Letters 42(2):542–549. doi: 10.1002/2014GL061957

Broecker WS, Sutherland S, Smethie W, Peng TH, Ostlund G. 1995. Oceanic radiocarbon: separation of the natural and bomb components. Global Biogeochemical Cycles 9:263–288. https://agupubs.onlinelibrary.wiley.com/doi/pdf/10.1029/95GB00208

Caldeira K, Rau GH, Duffy PB. 1998. Predicted net efflux of radiocarbon from the ocean and increase in atmospheric radiocarbon content. Geophysical Research Letters 25:3811–3814. https://agupubs.onlinelibrary.wiley.com/doi/pdf/10.1029/1998GL900010

Canadell JG, et al. 2021. Global carbon and other biogeochemical cycles and feedbacks. In: Masson-Delmotte V, et al. editors. Climate Change 2021: The Physical Science Basis. Contribution of Working Group I to the Sixth Assessment Report of the Intergovernmental Panel on Climate Change. Cambridge University Press, Cambridge, UK and New York, NY, USA. doi:10.1017/9781009157896.007. p. 673–816.

Dlugokencky E, Tans P. 2018. Trends in atmospheric carbon dioxide, edited, NOAA/ESRL http://www.esrl.noaa.gov/gmd/ccgg/trends/global.html

Donahue DJ, Linick T, Jull AT. 1990. Isotope-ratio and background corrections for accelerator mass spectrometry radiocarbon measurements. Radiocarbon 32:135–142.

Etheridge DM, Steele LP, Langenfelds RL, Francey RJ, Barnola JM, Morgan VI. 1996. Natural and anthropogenic changes in atmospheric CO_2 over the last 1000 years from air in Antarctic ice and firn. Journal of Geophysical Research: Atmospheres 101:4115–4128. doi: 10.1029/95JD03410

Etheridge DM, et al. 2010. Law Dome Ice Core 2000-Year CO_2, CH_4, and N_2O Data. IGBP PAGES/World Data Center for Paleoclimatology Data Contribution Series # 2010-070. NOAA/NCDC Paleoclimatology Program, Boulder CO, USA. https://www.ncei.noaa.gov/pub/data/paleo/icecore/antarctica/law/law2006.xls

Francey RJ, Allison CE, Etheridge DM, Trudinger CM, Enting IG, Leuenberger M, Langenfelds RL, Michel E, Steele LP. 1999. A 1000-year high precision record of $\delta^{13}C$ in atmospheric CO_2. Tellus B 51(2):170–193.

Godwin H. 1962. Half-life of radiocarbon. Nature 195:1984.

Graven HD. 2015. Impact of fossil fuel emissions on atmospheric radiocarbon and various applications of radiocarbon over this century. Proc. Nat. Acad. Sci. 112:9542–9545. https://www.pnas.org/content/112/31/9542

Graven HD, Guilderson TP, Keeling RF. 2012. Observations of radiocarbon in CO2 at seven global sampling sites in the Scripps flask network: analysis of spatial gradients and seasonal cycles. Journal of Geophysical Research 117. doi:10.1029/2011jd016535

Graven H, Allison CE, Etheridge DM, Hammer S, Keeling RF, Levin I, Meijer HAJ, Rubino M, Tans PP, Trudinger CM, Vaughn BH. 2017. Compiled records of carbon isotopes in atmospheric CO_2 for historical simulations in CMIP6. Geoscientific Model Development 10(12):4405–4417.

Hesshaimer V, Heimann M, Levin I. 1994. Radiocarbon evidence for a smaller oceanic carbon dioxide sink than previously believed. Nature 370(6486):201–203.

Hmiel B, Petrenko VV, Dyonisius MN, Buizert C, Smith AM, Place PF, Harth C, Beaudette R, Hua Q, Yang B, Vimont I. 2020. Preindustrial $^{14}CH_4$ indicates greater anthropogenic fossil CH_4 emissions. Nature 578(7795):409–412.

Hua Q, Turnbull JC, Santos GM, Rakowski AZ, Ancapichún S, De Pol-Holz R, Hammer S, Lehman SJ, Levin I, Miller JB, Palmer JG, Turney CSM. 2022. Atmospheric radiocarbon for the period 1950–2019. Radiocarbon 64:723–745.

Hughen K, Lehman S, Southon J, Overpeck J, Marchal O, Herring C, Turnbull J. 2004. ^{14}C activity and global carbon cycle changes over the past 50,000 years. Science 303:202–207.

Jöckel P, Brenninkmeijer CA, Lawrence MG, Jeuken AB, van Velthoven PF. 2002. Evaluation of stratosphere–troposphere exchange and the hydroxyl radical distribution in three-dimensional global atmospheric models using observations of cosmogenic ^{14}CO. Journal of Geophysical Research: Atmospheres. doi:10.1029/2001jd001324

Joos F, Bruno M. 1998. Long-term variability of the terrestrial and oceanic carbon sinks and the budgets of the carbon isotopes ^{13}C and ^{14}C. Global Biogeochemical Cycles 12(2):277–295.

Karlén I, Olsson IU, Kållburg P, Kilicci S. 1964. Absolute determination of the activity of two ^{14}C dating standards. Ark. Geofys. 4:465–471.

Keeling CD, Bacastow RB, Bainbridge AE, Ekdahl CA Jr., Guenther PR, Waterman LS, Chin JFS. 1976. Atmospheric carbon dioxide variations at Mauna Loa Observatory, Hawaii. Tellus 28(6):538–551. doi: 10.1111/j.2153-3490.1976.tb00701.x

Keeling CD, Piper SC, Bacastow RB, Wahlen M, Whorf TP, Heimann M, Meijer HAJ. 2001. Exchanges of atmospheric CO2 and $^{13}CO2$ with the terrestrial biosphere and oceans from 1978 to 2000. I. Global aspects, SIO Reference Series, No. 01-06, Scripps Institution of Oceanography, San Diego, 88 pages. http://scrippsco2.ucsd.edu

Key RM, Kozyr A, Sabine CL, Lee K, Wanninkhof R, Bullister JL, Feely RA, Millero FJ, Mordy C, Peng TH. 2004. A global ocean carbon climatology: results from Global Data Analysis Project (GLODAP). Global Biogeochemical Cycles. doi:10.1029/2004GB002247

Köhler P, Adolphi F, Butzin M, Muscheler R. 2022. Toward reconciling radiocarbon production rates with carbon cycle changes of the last 55,000 years. Paleoceanography and Paleoclimatology 37: e2021PA004314.

Lassey KR, Enting IG, Trudinger CM. 1996. The Earth's radiocarbon budget: a consistent model of the global carbon and radiocarbon cycles. Tellus B: Chemical and Physical Meteorology 48(4):487–501.

Lehman SJ, Miller JB, Wolak C, Southon JR, Tans PP, Montzka SA, Sweeney C, Andrews AE, LaFranchi BW, Guilderson TP, Turnbull JC. 2013. Allocation of terrestrial carbon sources using $^{14}CO_2$: Methods, measurement, and modelling. Radiocarbon 55:1484–1495.

https://doi.org/10.1017/RDC.2024.27 Published online by Cambridge University Press

Le Quéré C, et al. 2018. Global Carbon Budget 2017. Earth Syst. Sci. Data 10:405–448. doi: 10.5194/essd-10-405-2018

Levin I, Kromer B, Schoch-Fischer H, Bruns M, Münnich M, Berdau D, Vogel JC, Münnich KO. 1985. 25 years of tropospheric ^{14}C observations in central Europe. Radiocarbon 27(1):1–19.

Levin I, Kromer B, Francey RJ. 1996. Continuous measurements of ^{14}C in atmospheric CO2 at Cape Grim. In: Francey RJ, Dick AL, Derek N, editors. Baseline Atmospheric Program Australia 1994–1995. Melbourne: CSIRO. p 106–107.

Levin I, Kromer B, Francey RJ. 1999. Continuous measurements of ^{14}C in atmospheric CO2 at Cape Grim, 1995–1996. In: Grass JL, Derek N, Tindale NW, Dick AL, editors. Baseline Atmospheric Program Australia 1996. Melbourne: Bureau of Meteorology and CSIRO Atmospheric Research. p. 89–90.

Levin I, Naegler T, Kromer B, Diehl M, Francey R, Gomez-Pelaez A, Steele P, Wagenbach D, Weller R, Worthy D. 2010. Observations and modelling of the global distribution and long-term trend of atmospheric $^{14}CO_2$. Tellus B: Chemical and Physical Meteorology 62(1):26–46.

Levin I, Kromer B, Steele LP, Porter LW. 2011. Continuous measurements of ^{14}C in atmospheric CO2 at Cape Grim, 1997–2008. In: Derek N, Krummel PB, editors. Baseline Atmospheric Program Australia 2007–2008. Melbourne: Australian Bureau of Meteorology and CSIRO Marine and Atmospheric Research. p. 56–59.

MacFarling Meure C. 2004. The natural and anthropogenic variations of carbon dioxide, methane and nitrous oxide during the Holocene from ice core analysis. PhD thesis, University of Melbourne.

MacFarling Meure C, Etheridge D, Trudinger C, Steele P, Langenfelds R, van Ommen T, Smith A, Elkins J. 2006. The Law Dome CO_2, CH_4 and N_2O Ice Core Records Extended to 2000 years BP. Geophysical Research Letters 33(14):L14810. doi: 10.1029/2006GL026152.

Manning MR, Lowe DC, Moss RC, Bodeker GE, Allan W. 2005. Short-term variations in the oxidizing power of the atmosphere. Nature 436:1001–1004. doi: 10.1038/nature03900.

Millard AR. 2014. Conventions for reporting radiocarbon determinations. Radiocarbon 56: 555–559.

Mook W, Van der Plicht J. 1999. Reporting ^{14}C activities and concentrations. Radiocarbon 41(3):227–239. doi: 10.1017/S0033822200057106

Mouchet A. 2013. The ocean bomb radiocarbon inventory revisited. Radiocarbon 55:1580–1594. doi: 10.2458/azu_js_rc.55.16402.

Naegler T, Levin I. 2006. Closing the global radiocarbon budget 1945–2005. J. Geophys. Res. 111:D12311. doi: 10.1029/2005JD006758

Peacock S. 2004. Debate over the ocean bomb radiocarbon sink: closing the gap. Global Biogeochem. Cycles 18:GB2022. doi: 10.1029/2003GB002211

Prather MJ, Holmes CD, Hsu J. 2012. Reactive greenhouse gas scenarios: systematic exploration of uncertainties and the role of atmospheric chemistry. Geophysical Research Letters 39(9). doi: 10.1029/2012GL051440

Reimer PJ, Brown TA, Reimer RW. 2004. Discussion: reporting and calibration of post-bomb C-14 data. Radiocarbon 46:1299–304.

Roth R, Joos F. 2013. A reconstruction of radiocarbon production and total solar irradiance from the Holocene ^{14}C and CO_2 records: implications of data and model uncertainties. Climate of the Past 9:1879–1909. doi: 10.5194/cp-9-1879-2013

Schwartz SE, Keeling RF, Meijer HAJ, Turnbull JC. 2022. Comment on "World Atmospheric CO_2, Its ^{14}C Specific Activity, Non-fossil Component, Anthropogenic Fossil Component, and Emissions (1750–2018)," by Kenneth Skrable, George Chabot, and Clayton French. Health Physics 122:717–719. https://journals.lww.com/health-physics/Fulltext/2022/06000/Comment_on__World_Atmospheric_CO2,_Its_14C.13.aspx

Stuiver M. 1980. Workshop on ^{14}C data reporting. Radiocarbon 22(3):964–966.

Stuiver M, Polach HA. 1977. Discussion. Reporting of ^{14}C data. Radiocarbon 19:355–363. https://journals.uair.arizona.edu/index.php/radiocarbon/article/viewFile/4183/3608

Stuiver M, Quay PD. 1981. Atmospheric ^{14}C changes resulting from fossil fuel CO_2 release and cosmic ray flux variability. Earth and Planetary Science Letters 53(3):349–362. https://www.sciencedirect.com/science/article/abs/pii/0012821X81900406

Stuiver M, Reimer PJ, Braziunas TF. 1998. High-precision radiocarbon age calibration for terrestrial and marine samples. Radiocarbon 40:1127–1151. https://www.cambridge.org/core/journals/radiocarbon/article/highprecisionradiocarbon-age-calibration-for-terrestrial-and-marine-samples/1660E9D7A43772ACBB56614C1DD09D46

Suess HE. 1955. Radiocarbon concentration in modern wood. Science 122(3166):415–417.

Turnbull J, Rayner P, Miller J, Naegler T, Ciais P, Cozic A. 2009. On the use of $^{14}CO_2$ as a tracer for fossil fuel CO_2: Quantifying uncertainties using an atmospheric transport model. Journal of Geophysical Research: Atmospheres 114(D22).

Turnbull JC, Mikaloff Fletcher SE, Ansell I, Brailsford GW, Moss RC, Norris MW, Steinkamp K. 2017. Sixty years of radiocarbon dioxide measurements at Wellington, New Zealand: 1954–2014. Atmospheric Chemistry and Physics 17:14771–14784. doi: 10.5194/acp-17-14771-2017.

https://doi.org/10.1017/RDC.2024.27 Published online by Cambridge University Press

Wu Y, Fallon SJ, Cantin NE, Lough JM. 2021. Surface ocean radiocarbon from a Porites coral record in the Great Barrier Reef: 1945–2017. Radiocarbon 63:1193–1203.

Yang X, North R, Romney C. 2000. CMR nuclear explosion database (revision 3), CMR Tech. Rep. 00/16, Cent. for Monitor. Res., U. S. Army Space and Missile Defense Command, Arlington, VA. https://www.ldeo.columbia.edu/~richards/my_papers/WW_nuclear_tests_IASPEI_HB.pdf (downloaded 2020-0119).

APPENDIX A
Relation of measured activity of atmospheric CO_2, reported as atmospheric $\Delta^{14}CO_2$, and absolute amount of atmospheric $^{14}CO_2$

The expression for conversion of measured $\Delta^{14}CO_2$ to x_{14CO2} given as Eq. (1) of the main text and presented earlier by Karlén et al. 1964 and Stuiver 1980,

$$x_{14CO2} = f\left[\frac{1+\delta^{13}CO_2}{1-0.025}\right]^2(1+\Delta^{14}CO_2)x_{CO_2}, \tag{1}$$

is developed here. The quantities Δ and δ, representing departure of isotopic ratio from that of a standard are given as decimal fractions; e.g., for $\Delta^{14}CO_2 = 1‰$, the value in the conversion expression is 0.001. The factor

$$f \equiv \frac{M_C A^{ABS}}{\lambda N_A} = 1.176 \times 10^{-12} \tag{A1}$$

is a constant; M_C is the molecular weight of carbon, A^{ABS} is the activity of the absolute standard, λ is the decay constant of ^{14}C, and N_A is the Avogadro constant.

The relation between the amount of $^{14}CO_2$ in a sample and the relative activity of ^{14}C in the sample reported as $\Delta^{14}C$ follows the conventions of Stuiver and Polach (1977) and Stuiver (1980). These conventions, which were developed initially for reporting $\Delta^{14}C$ from activity measurements, have since been adapted for application to the now more widely used accelerator mass spectrometry (AMS) approach (Donahue et al. 1990; Mook and van der Plicht 1999). From Stuiver (1980, Eq. 1) the depletion or enrichment of ^{14}C relative to an absolute standard corrected for mass-dependent fractionation is defined as

$$\Delta^{14}C = (1+\delta^{14}C)\left[\frac{1-0.025}{1+\delta^{13}C}\right] - 1, \tag{A2}$$

where $\delta^{13}C$ and $\delta^{14}C$ denote the fractional depletion or enrichment with respect to the respective standards. Combining Eq. (A2) with the expression relating $\delta^{14}C$ to the specific activities of the absolute standard and the air sample, A^{ABS} and A^S, respectively (Stuiver and Polach 1977)

$$\delta^{14}C = \frac{A^S e^{\lambda(y-x)}}{A^{ABS}} - 1, \tag{A3}$$

where A^{ABS}= 0.226 Bq g(C) $^{-1}$ (Mook and van der Plicht 1999), λ is the decay constant of ^{14}C (3.8332×10^{-12} s^{-1}) corresponding to a geophysical half-life of 5730 ± 40 years (Godwin 1962) and x and y denote year of growth (for tree-ring samples) and year of measurement, respectively, yields specific activity of an air sample A^S in terms of $\Delta^{14}CO_2$ and $\delta^{13}CO_2$ as

https://doi.org/10.1017/RDC.2024.27 Published online by Cambridge University Press

$$A^{S} = A^{ABS}(1 + \Delta^{14}CO_2)\left[\frac{1 + \delta^{13}CO_2}{1 - 0.025}\right]^2 = gA^{ABS}(1 + \Delta^{14}CO_2). \tag{A4}$$

The factor g in Eq. (A4), defined as

$$g = \left[\frac{1 + \delta^{13}CO_2}{1 - 0.025}\right]^2 \approx 1.0373, \tag{A5}$$

accounts for fractionation, where the numerical value (1.0373) is for $\delta^{13}CO_2$ taken as –7‰. As that value of $\delta^{13}CO_2$ is representative for the past several centuries (e.g., Francey et al. 1999; Levin et al. 2010; Graven et al. 2017), the factor g can, to good approximation, be treated as constant, as seen by the near equality of the red and green data points in Figures 1b and 2 of the main text. For the range of $\delta^{13}CO_2$ from preindustrial time to the present, –6.4‰ to –8.4‰, the corresponding range of g is 1.0385 to 1.0343, Appendix B), supporting the use of a constant value of g if measurements of $\delta^{13}CO_2$ are not available. For precise work, such as comparison of x^{air}_{14CO2} at different locations (e.g., Figure 3), variation of g would need to be taken into account.

Noting that the number of ^{14}C atoms in a given sample $n^{S}_{14C} = A^{S}m^{S}_{C}/\lambda$, where m^{S}_{C} is the mass of carbon in the sample and that the number of carbon atoms in the sample $n^{S}_{C} = m^{S}_{C}N_A/M_C$, where N_A is the Avogadro constant (6.022×10^{23} mol^{-1}) and M_C is the molecular weight of carbon (12.011 g mol^{-1}) yields

$$n^{S}_{14C} = \frac{M_C A^{ABS}}{\lambda N_A} g(1 + \Delta^{14}C^{S})n^{S}_{C} = fg(1 + \Delta^{14}C^{S})n^{S}_{C,} \tag{A6a}$$

where the factor f, Eq. (A1), is a constant. Specializing to the amount of $^{14}CO_2$ in the global atmosphere, as mole fraction in dry air is proportional to number of molecules,

$$x_{14CO2} = fg(1 + \Delta^{14}CO_2)x_{CO_2} = f\left[\frac{1 + \delta^{13}CO_2}{1 - 0.025}\right]^2(1 + \Delta^{14}CO_2)x_{CO_2}, \tag{A6b}$$

as has been given previously, e.g., Karlén et al. (1964) and Stuiver (1980).

For $\delta^{13}CO_2 = -7$‰ the product $fg \approx 1.220 \times 10^{-12}$, the inverse of which was presented by Levin et al. (2010); this quantity is accurate to about 1% (Stuiver 1980). For present (2022) dry-air mole fraction of atmospheric CO_2, x_{CO2}, $\sim 420 \times 10^{-6}$ (420 parts per million, ppm) and $\Delta^{14}CO_2 \approx 0$, the mole fraction of atmospheric $^{14}CO_2$, x_{14CO2}, is approximately 512×10^{-18} (512 amol mol^{-1}), where amol mol^{-1} denotes attomoles (10^{-18} mol) per mole.

APPENDIX B

In addition to the dominant dependence of x_{14CO2} on $\Delta^{14}C$ and x_{CO2}, the fractionation factor g (Appendix A, Eq. A5), which is inferred from the amount of $^{13}CO_2$ in the sample $\delta^{13}CO_2$, exhibits a slight dependence on this amount, Figure B1. Although this dependence is slight, the systematic decrease in g of about 0.4% over the industrial era, Figure B2, should be accounted for in evaluation of x_{14CO2} in precise work, rather than simply using a constant value of $\delta^{13}CO_2$.

https://doi.org/10.1017/RDC.2024.27 Published online by Cambridge University Press

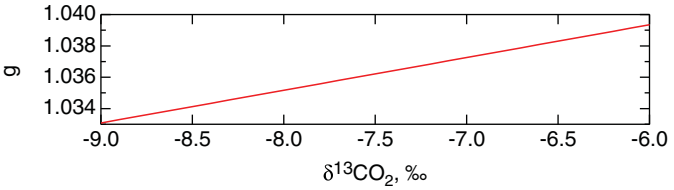


Figure B1 Dependence on $\delta^{13}CO_2$ of isotopic fractionation factor g required for evaluation of x_{14CO2} (Appendix A, Eq. A5).

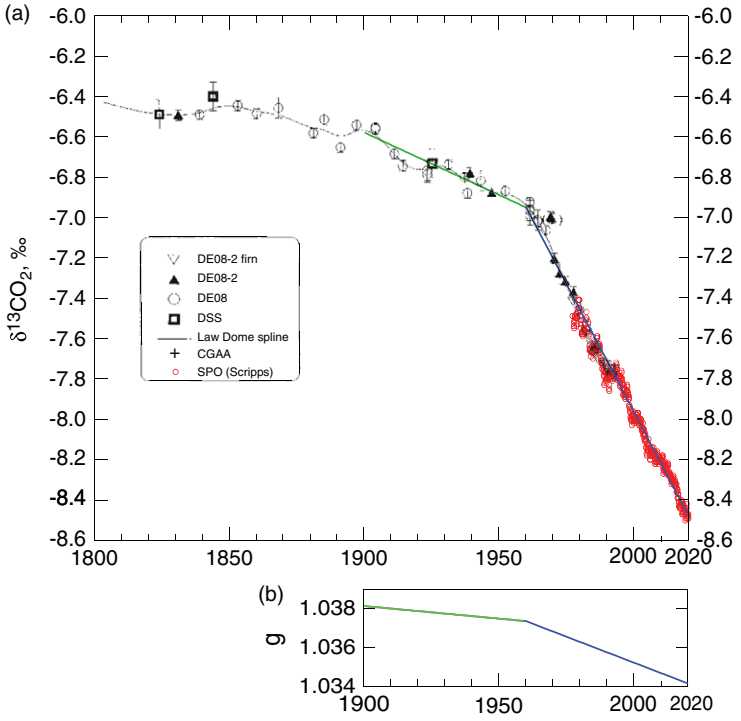


Figure B2 *a*. Time dependence of $\delta^{13}C$ of atmospheric CO_2 as compiled by Francey et al. (1999), data points and associated uncertainties are from the Cape Grim Air Archive, firn at DE08-2, and cores DE08, DE08-2 and DSS, Law Dome, Antarctica; thin black curve denotes spline fit. Red points denote measurements by Scripps Institution of Oceanography (Keeling et al. 2001; https://scrippsco2.ucsd.edu/assets/data/atmospheric/stations/flask_isotopic/monthly/monthly_flask_c13_spo.csv. Downloaded 2022-0811). Green and blue lines in panel *a* denote values of $\delta^{13}C$ employed in evaluation of isotopic fractionation factor g (panel *b*) used in evaluation of x_{14CO2} presented in Figures 1 and 2.

https://doi.org/10.1017/RDC.2024.27 Published online by Cambridge University Press